Electronic Supplementary Material (ESI) for Dalton transactions.
This journal is © The Royal Society of Chemistry 2023.

Electronic Supplementary Information

General Synthesis of $CoCeMO_x$ trimetallic oxides via cation exchange reaction for efficient oxygen evolution reaction

Xianggang Huang,[‡a] Xin Wang,[‡b] Yingxin Liu,[a] Yan Hou,[a] Chengjin Li,[c] Mingyang Cai,[a] Hongwei Gu[a] and Xueqin Cao[*a]

a Key Laboratory of Organic Synthesis of Jiangsu Province, College of Chemistry, Chemical Engineering and Materials Science and Collaborative Innovation Center of Suzhou Nano Science and Technology, Soochow University, Suzhou 215123, P. R. China.

b Key Laboratory of Rare Mineral of hubei Province, Ministry of Natural Resources, Hubei Geological Experimental Testing Center, Wuhan 430034, P. R. China.

c National Engineering Laboratory for Modern Silk, College of Textile and Clothing Engineering, Soochow University, Suzhou 215123, China

[‡] These authors contributed equally.

* Corresponding author:

E-mail: xqcao2022@sina.com

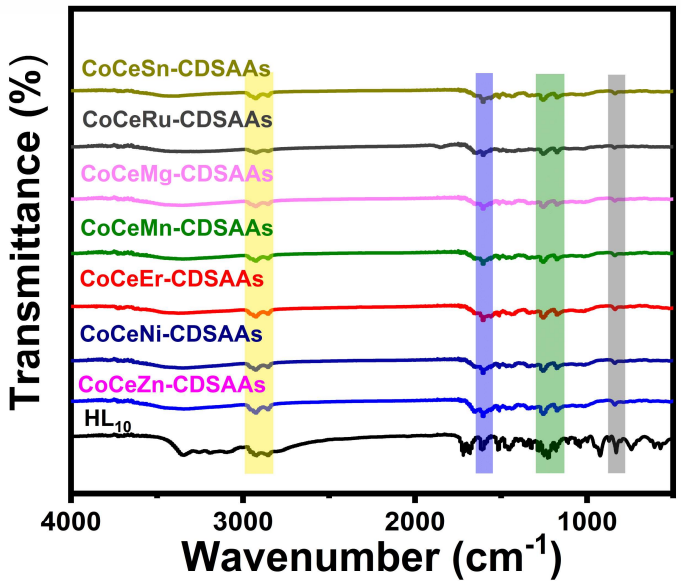

Figure S1 FT-IR patterns of HL_{10} and CoCeM-CDSAAs (M=Zn, Ni, Er, Mn, Mg, Ru and Sn).

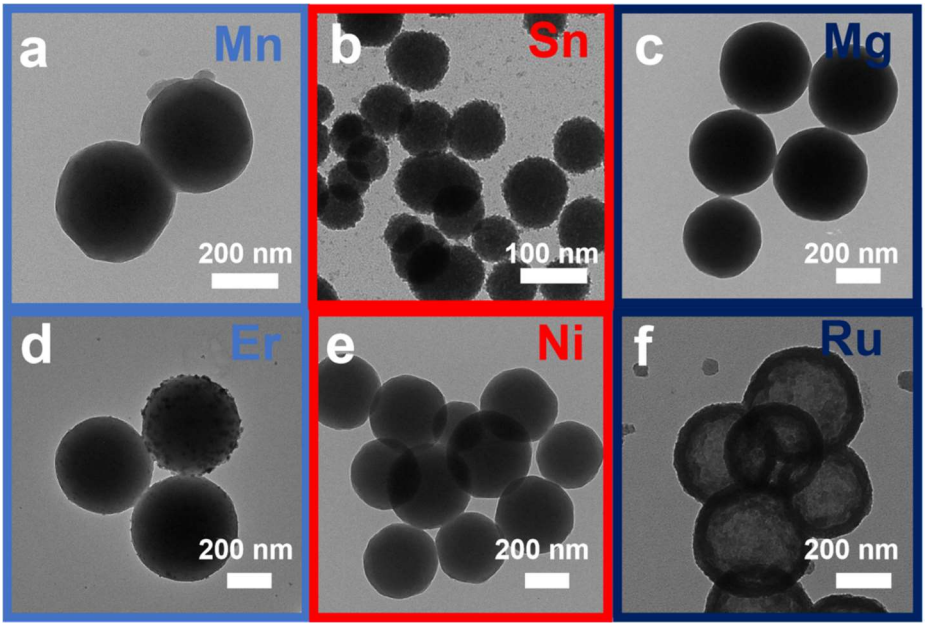

Figure S2 TEM images of (a) CoCeMn-CDSAAs, (b) CoCeSn-CDSAAs, (c) CoCeMg-CDSAAs, (d) CoCeEr-CDSAAs, (e) CoCeNi-CDSAAs and (f) CoCeRu-CDSAAs.

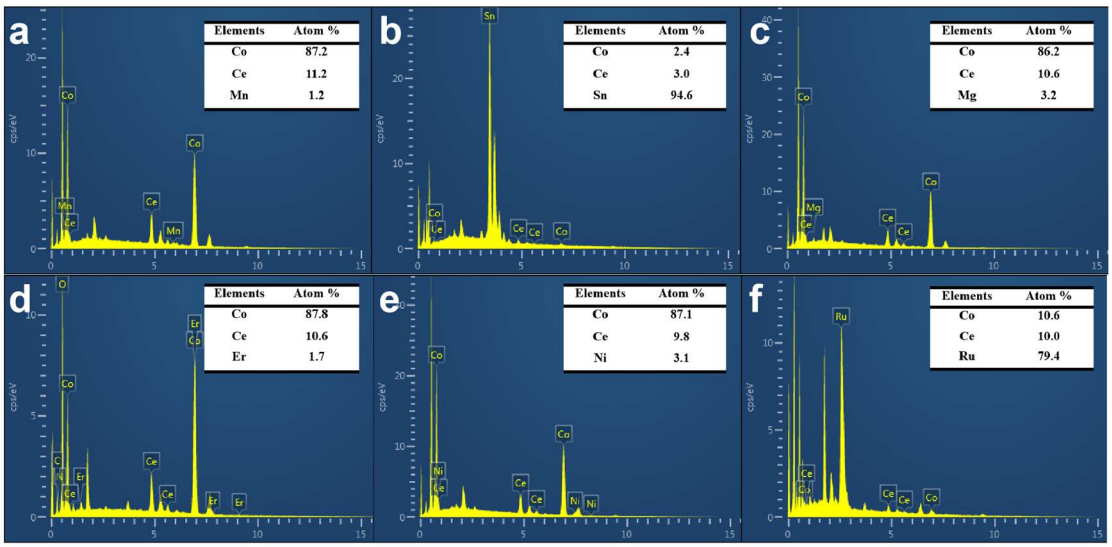

Figure S3 EDX images of (a) $CoCeMnO_x$ PNs, (b) $CoCeSnO_x$ PSNs, (c) $CoCeMgO_x$ HNs, (d) $CoCeErO_x$ PNs, (e) $CoCeNiO_x$ PSNs and (f) $CoCeRuO_x$ HNs.

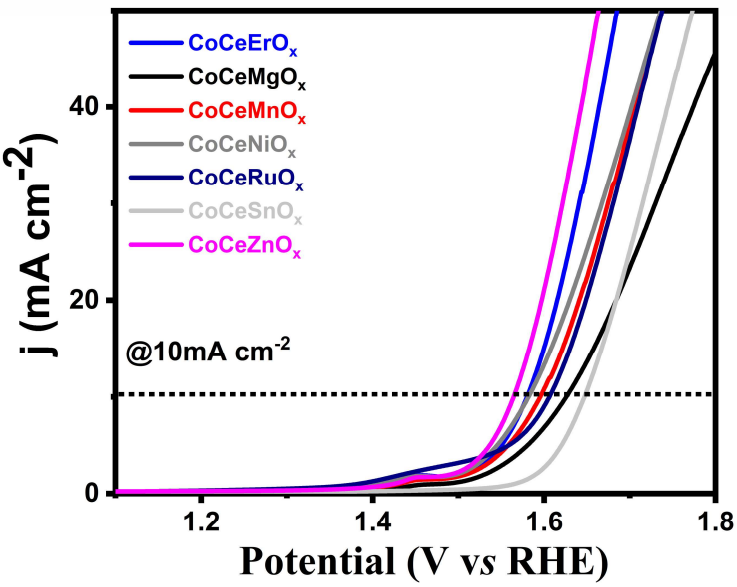

Figure S4 LSV curves of $CoCeMO_x$ (M=Zn, Ni, Er, Mn, Mg, Ru and Sn) for OER in 1 M KOH solution.

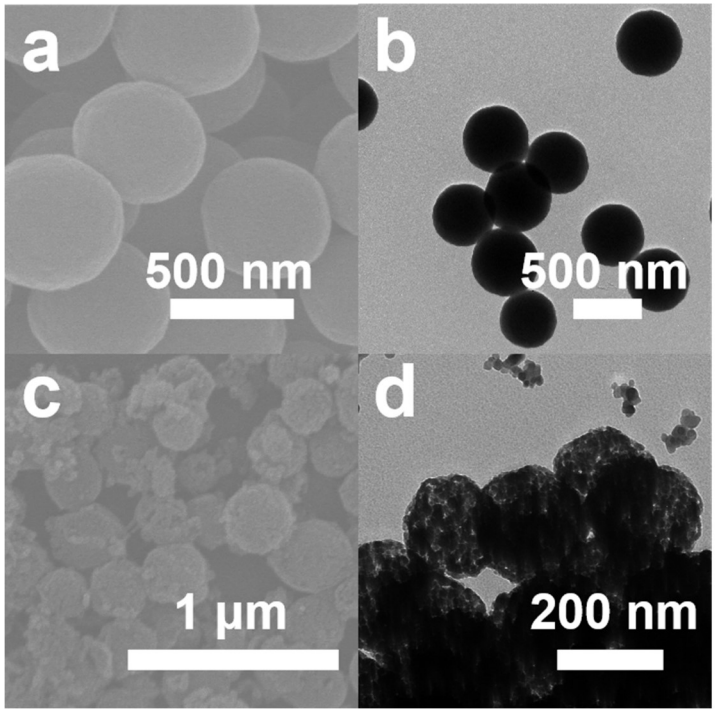

Figure S5 SEM and TEM images of (a, b) Co-CDSAAs, (c, d) Co-Oxides.

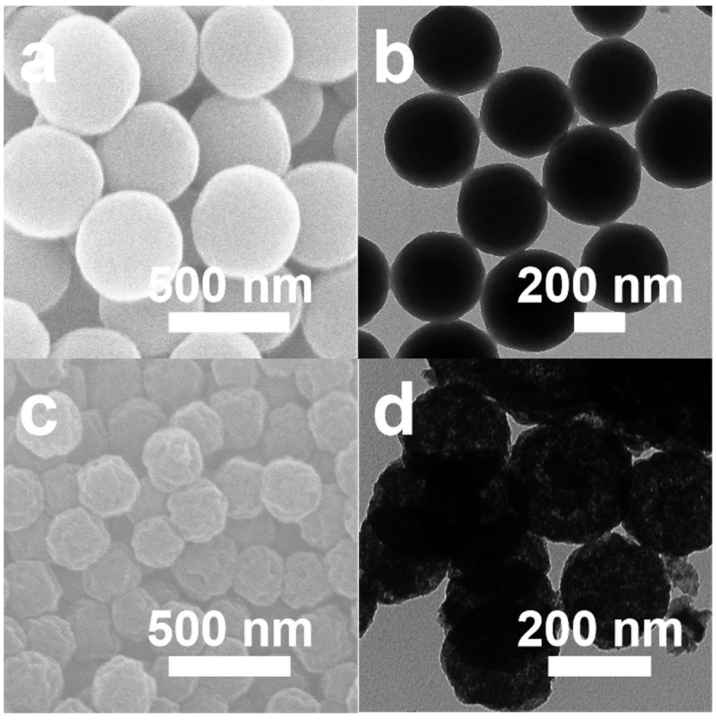

Figure S6 SEM and TEM images of (a, b) CoCe-CDSAAs, (c, d) CoCe-Oxides

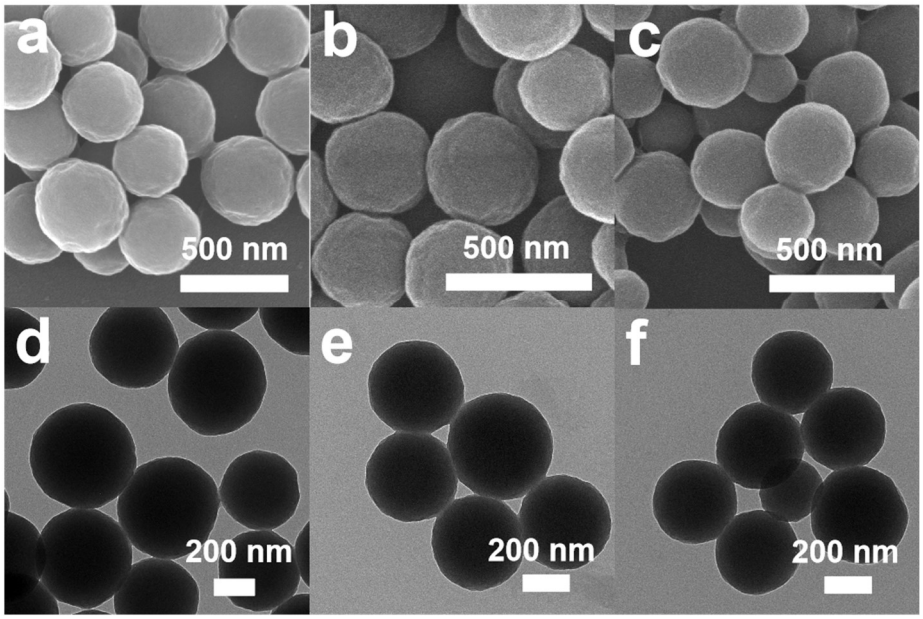

Figure S7 SEM and TEM images of (a, d) CoCe-CDSAAs-1, (b, e) CoCe-CDSAAs-2, (c, f) CoCe-CDSAAs-4.

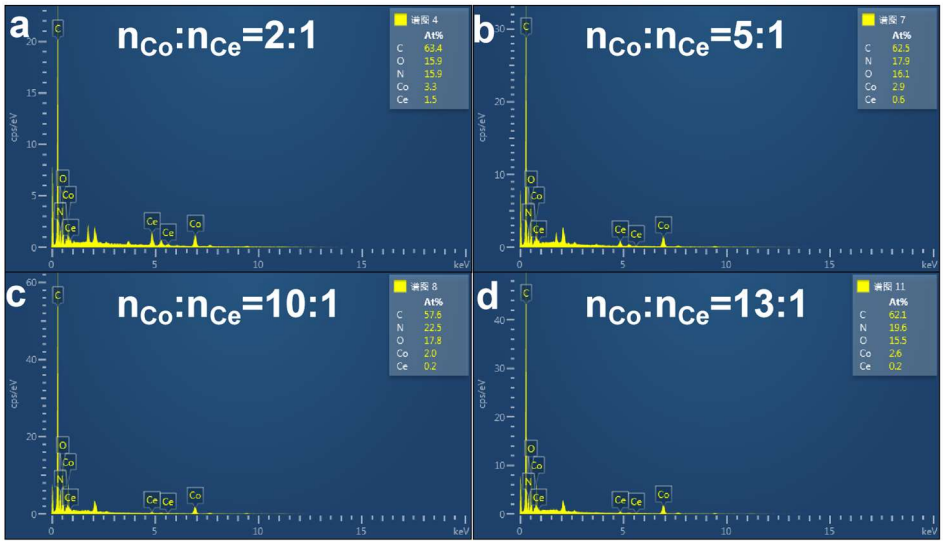

Figure S8 EDX data of (a) CoCe-CDSAAs-1, (b) CoCe-CDSAAs-2, (c) CoCe-CDSAAs, (d) CoCe-CDSAAs-4.

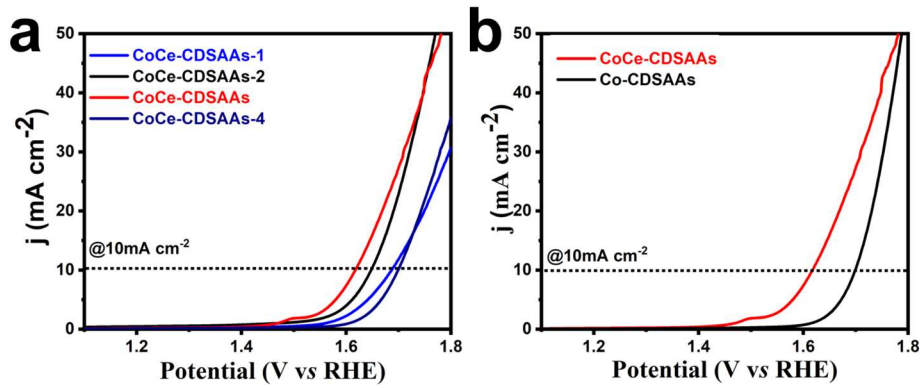

Figure S9 LSV curves in 1 M KOH solution for OER of (a) CoCe-CDSAAs-1, CoCe-CDSAAs-2, CoCe-CDSAAs, CoCe-CDSAAs-4, (b) CoCe-CDSAAs and Co-CDSAAs.

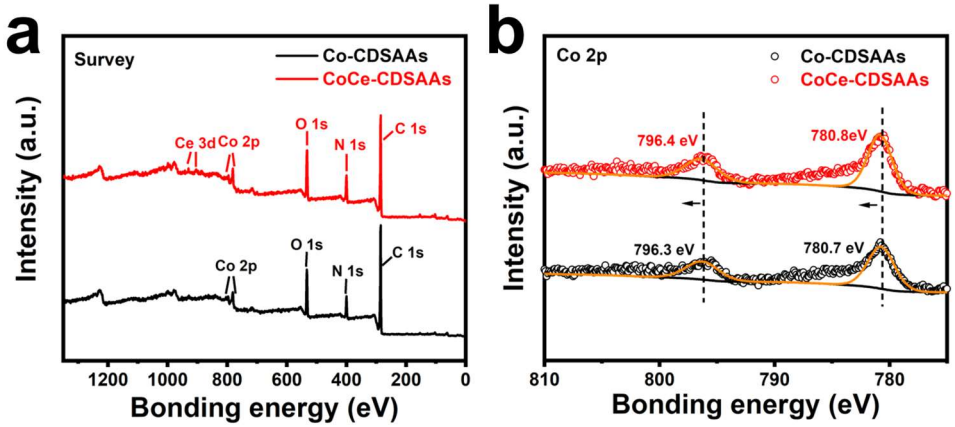

Figure S10 Survey spectra (a) and high High-resolution XPS spectra of (b) Co 2p for Co-CDSAAs and CoCe-CDSAAs.

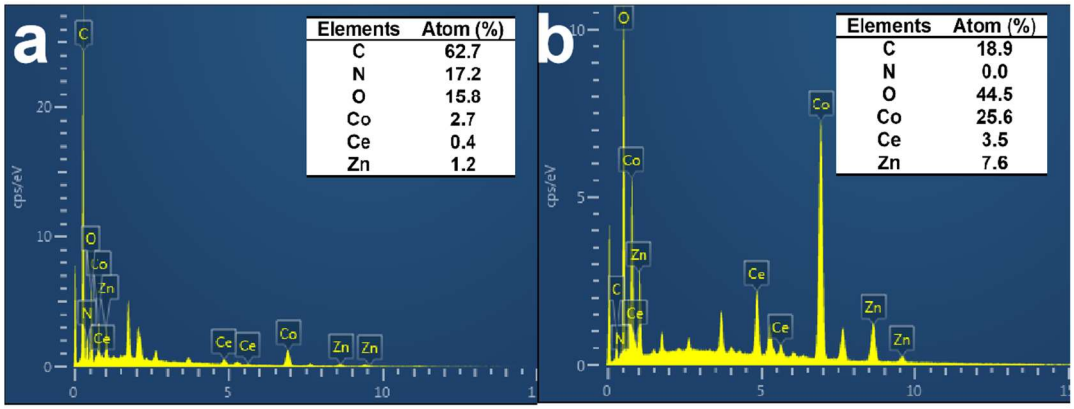

Figure S11 EDX images of (a) CoCeZn-CDSAAs and (b) $CoCeZnO_x$ PNs.

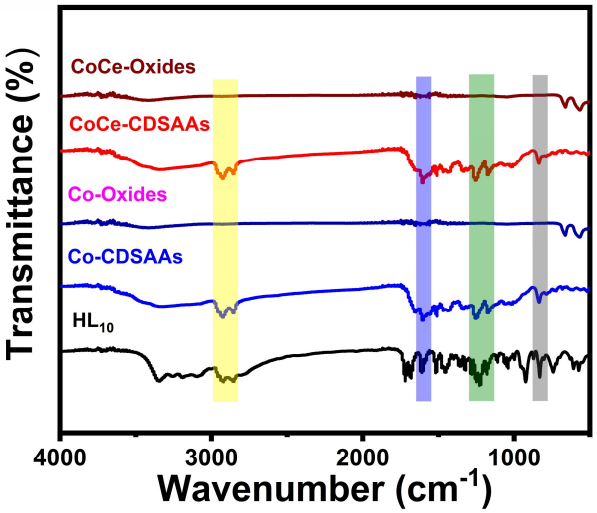

Figure S12 FI-IR patterns of HL_{10}, Co-CDSAAs, Co-Oxides, CoCe-CDSAAs and CoCe-Oxides.

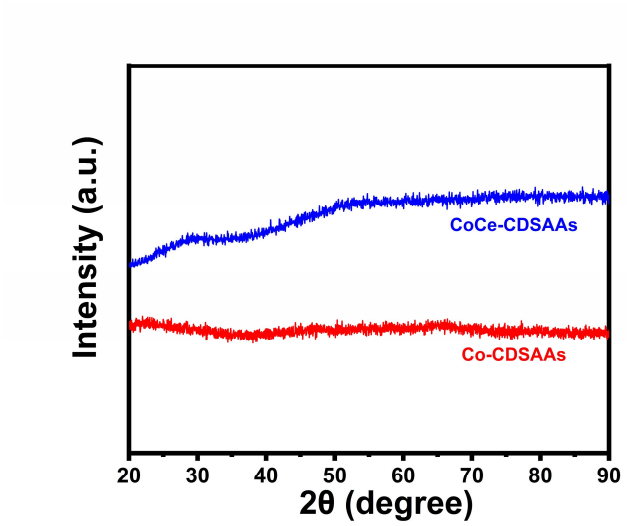

Figure S13 XRD patterns of Co-CDSAAs and CoCe-CDSAAs.

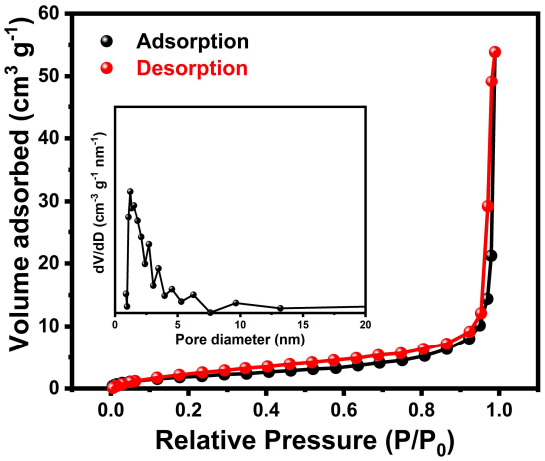

Figure S14 Nitrogen adsorption-desorption isotherms with inserted pore size distribution plots of CoCeZn-CDSAAs.

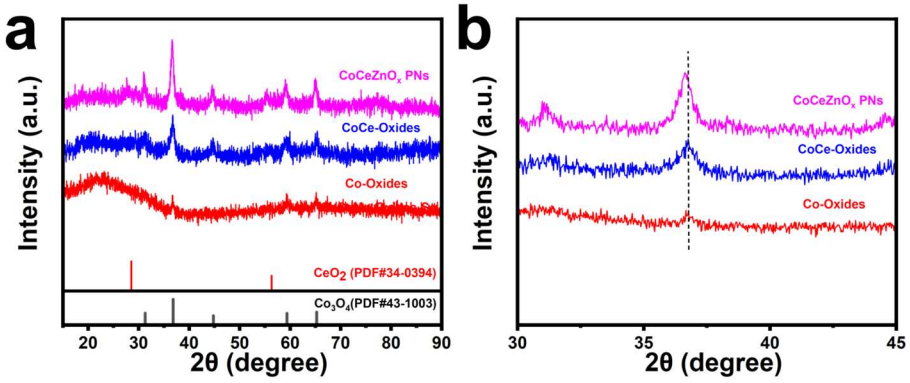

Figure S15 XRD (a) of $CoCeZnO_x$ PNs, CoCe-Oxides and Co-Oxides. Corresponding Magnified XRD patterns (b) in (311) of Co_3O_4.

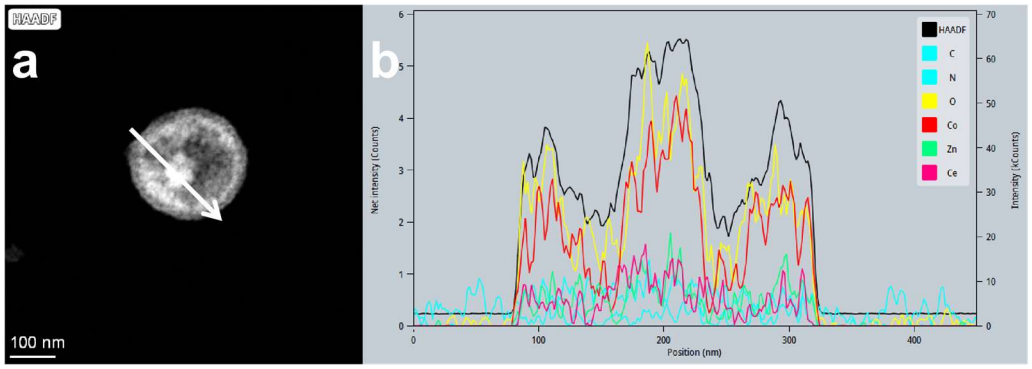

Figure S16 HAADF-STEM image (a) and EDX line scan image (b) of $CoCeZnO_x$ PNs.

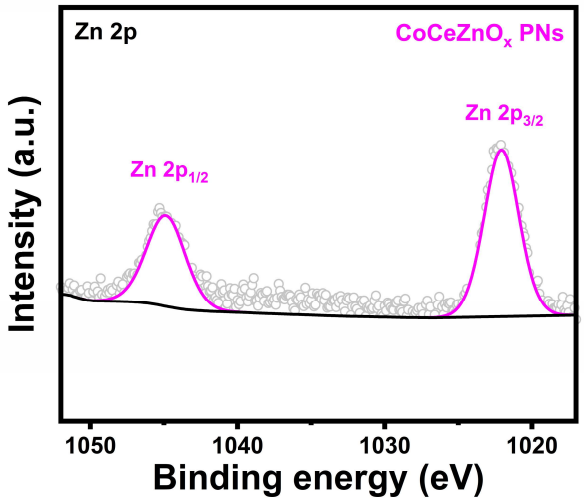

Figure S17 High-resolution XPS spectra of Zn2p in $CoCeZnO_x$ PNs.

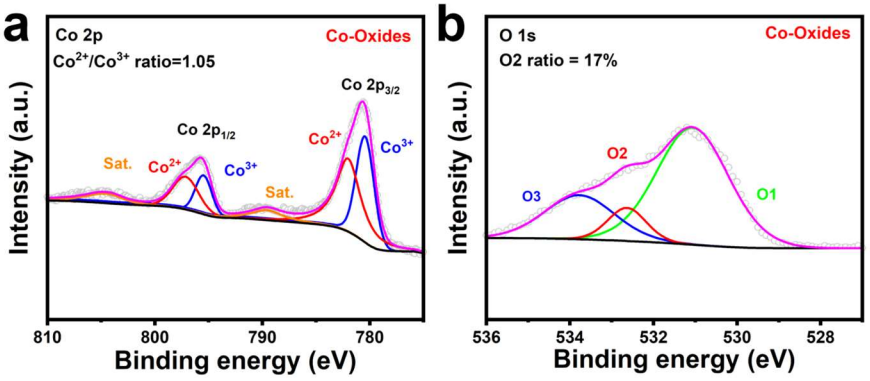

Figure S18 High-resolution XPS spectra of (a) Co2p and (b) O1s in Co-Oxides.

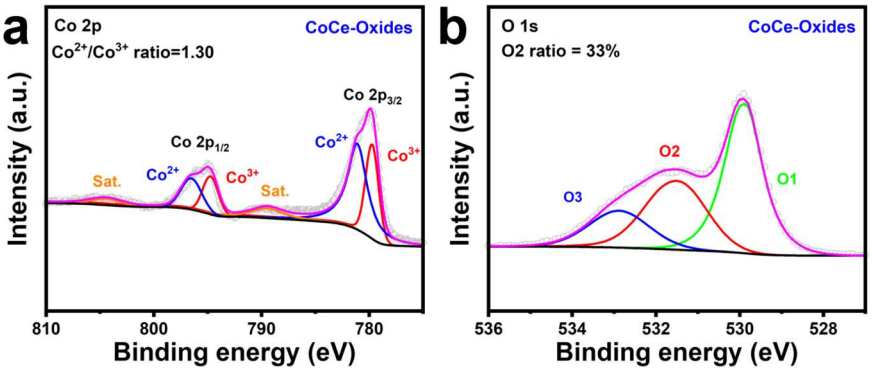

Figure S19 High-resolution XPS spectra of (a) Co2p and (b) O1s in CoCe-Oxides.

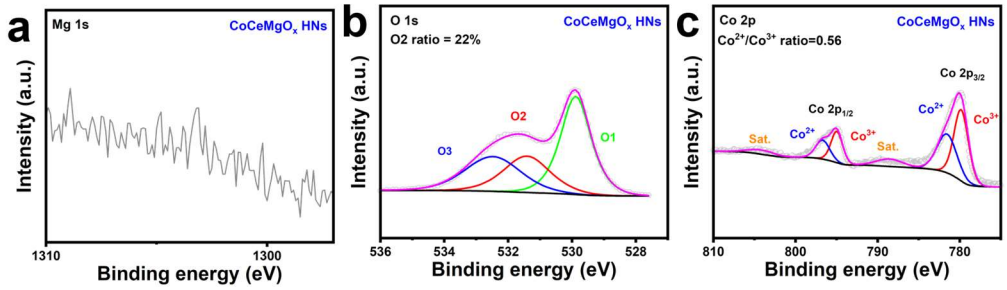

Figure S20 (a) Mg 1s, (b) O 1s and (c) Co 2p high-resolution XPS spectra in $CoCeMgO_x$ HNs.

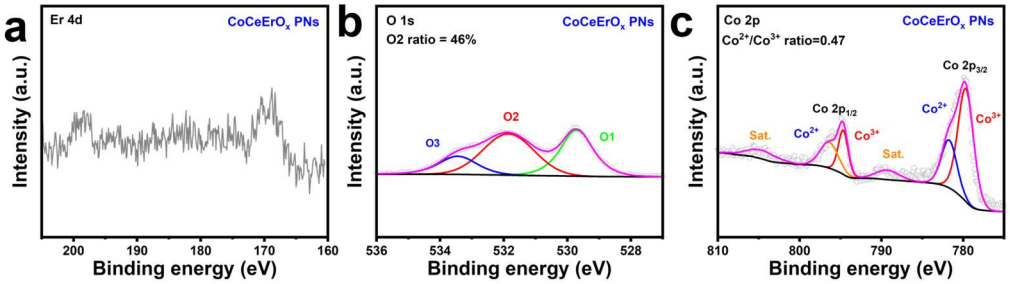

Figure S21 (a) Er 4d, (b) O 1s and (c) Co 2p high-resolution XPS spectra in $CoCeErO_x$ PNs.

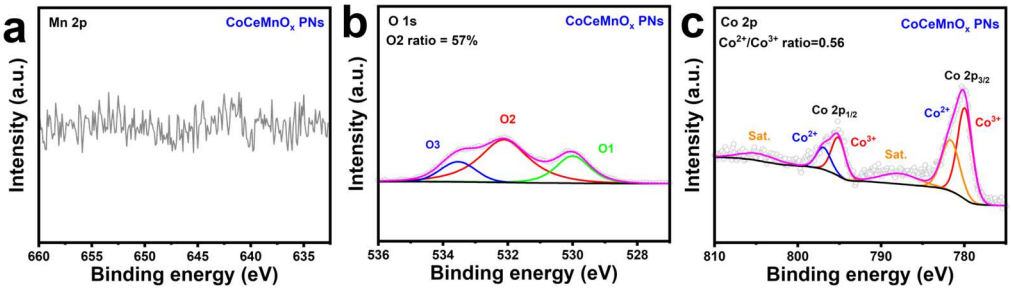

Figure S22 (a) Mn 2p, (b) O 1s and (c) Co 2p high-resolution XPS spectra in $CoCeMnO_x$ PNs.

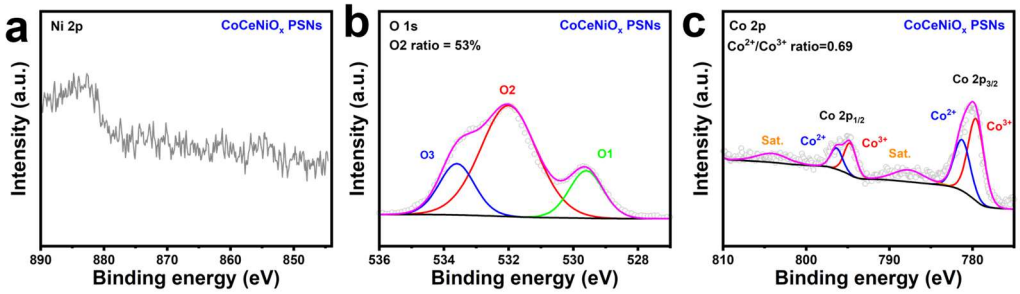

Figure S23 (a) Ni 2p, (b) O 1s and (c) Co 2p high-resolution XPS spectra in $CoCeNiO_x$ PSNs.

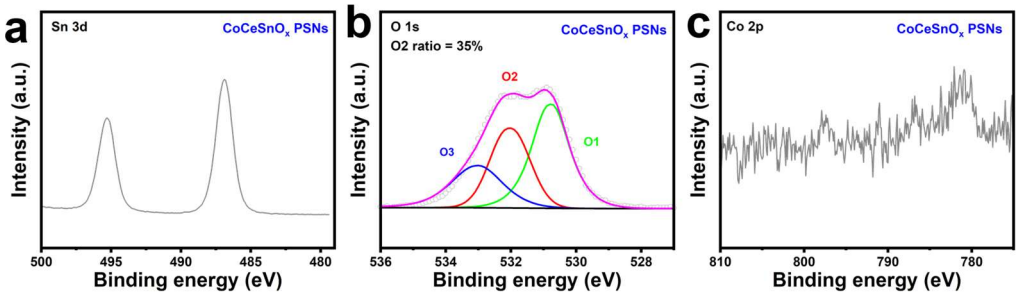

Figure S24 (a) Sn 3d, (b) O 1s and (c) Co 2p high-resolution XPS spectra in $CoCeSnO_x$ PSNs.

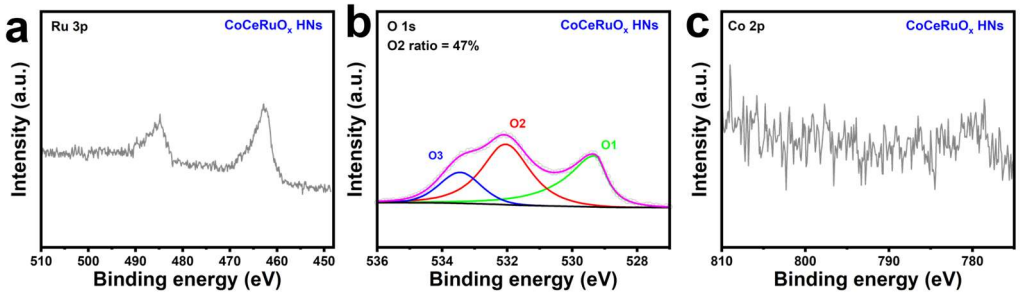

Figure S25 (a) Ru 3p, (b) O 1s and (c) Co 2p high-resolution XPS spectra in $CoCeRuO_x$ HNs.

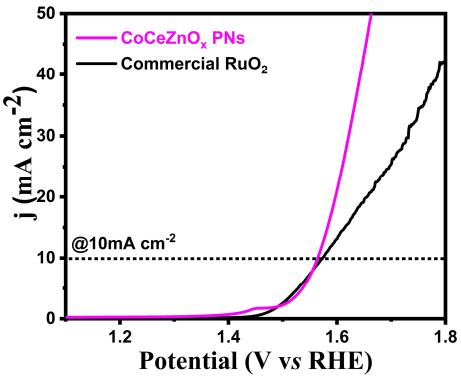

Figure S26 LSV curves of Commercial RuO_2 in 1 M KOH solution.

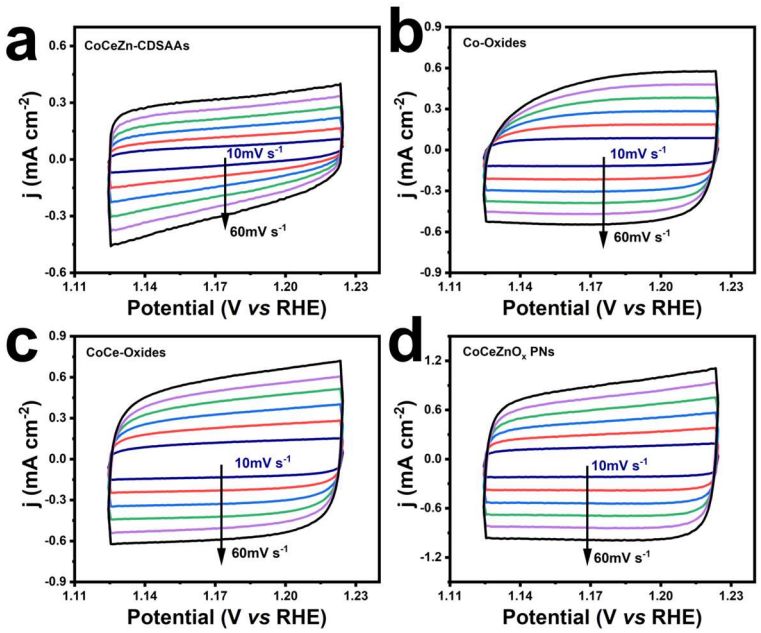

Figure S27 CV curves of (a) CoCeZn-CDSAAS, (b) CoOxides, (c) CoCe-Oxides and (d) CoCeZnOx PNs with different scan rates from 10 to 60 mV s^{-1}.

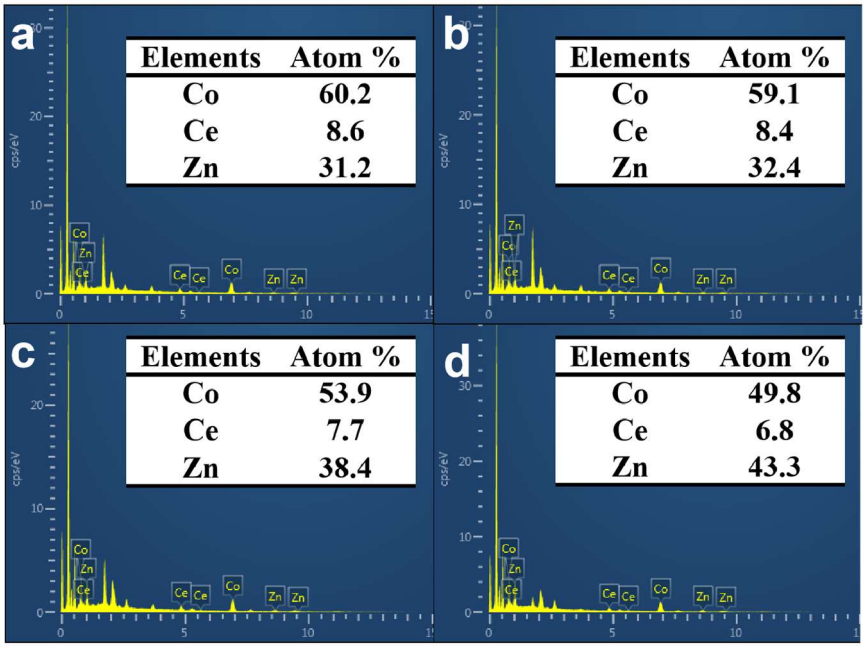

Figure S28 EDX images of (a) CoCeZn-CDSAAs-1 (3mL $ZnCl_2$), (b) CoCeZn-CDSAAs-2 (7mL $ZnCl_2$), (c) CoCeZn-CDSAAs (11mL $ZnCl_2$) and (d) CoCeZn-CDSAAs-4 (20mL $ZnCl_2$).

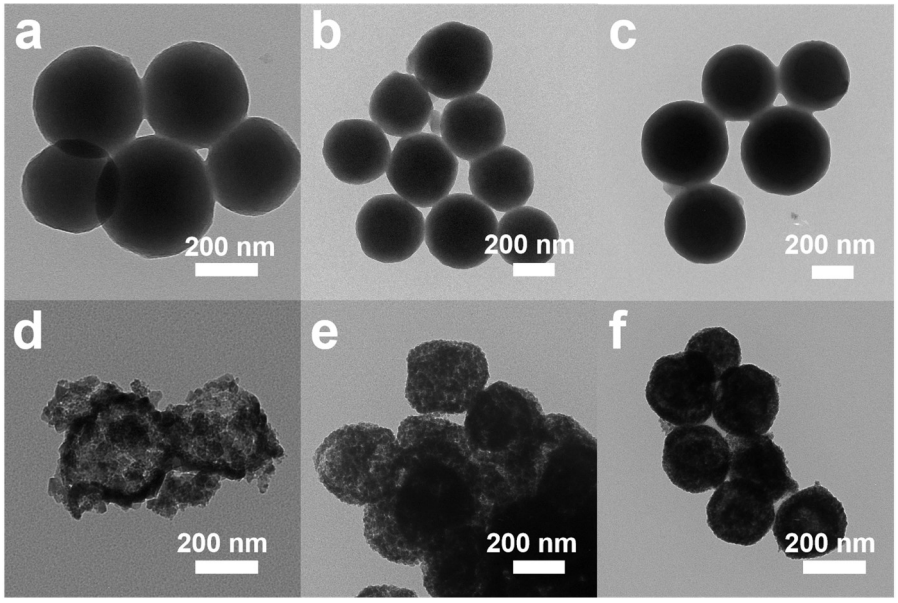

Figure S29 TEM images of (a) CoCeZn-CDSAAs-1, (b) CoCeZn-CDSAAs-2, (c) CoCeZn-CDSAAs-4, (d) $CoCeZnO_x$-1, (e) $CoCeZnO_x$-2 and (f) $CoCeZnO_x$-4.

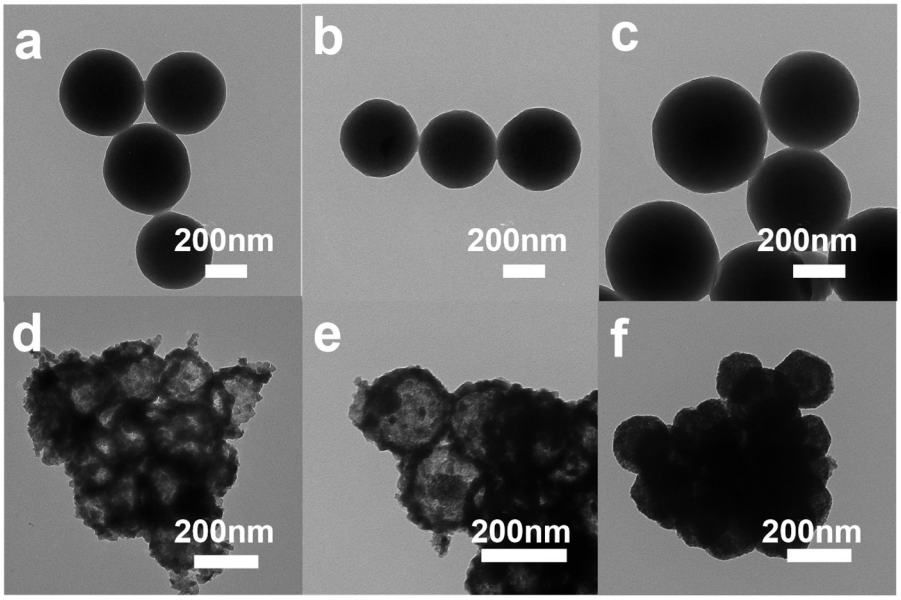

Figure S30 TEM images of (a) CoCeMg-CDSAAs-1, (b) CoCeMg-CDSAAs-2, (c) CoCeMg-CDSAAs-4, (d) $CoCeMgO_x$-1, (e) $CoCeMgO_x$-2 and (f) $CoCeMgO_x$-4.

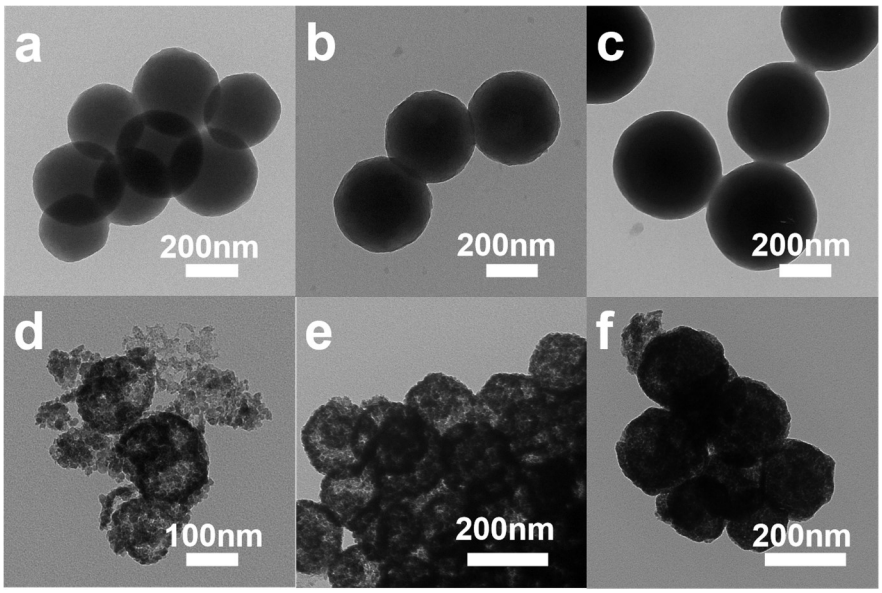

Figure S31 TEM images of (a) CoCeMn-CDSAAs-1, (b) CoCeMn-CDSAAs-2, (c) CoCeMn-CDSAAs-4, (d) $CoCeMnO_x$-1, (e) $CoCeMnO_x$-2 and (f) $CoCeMnO_x$-4.

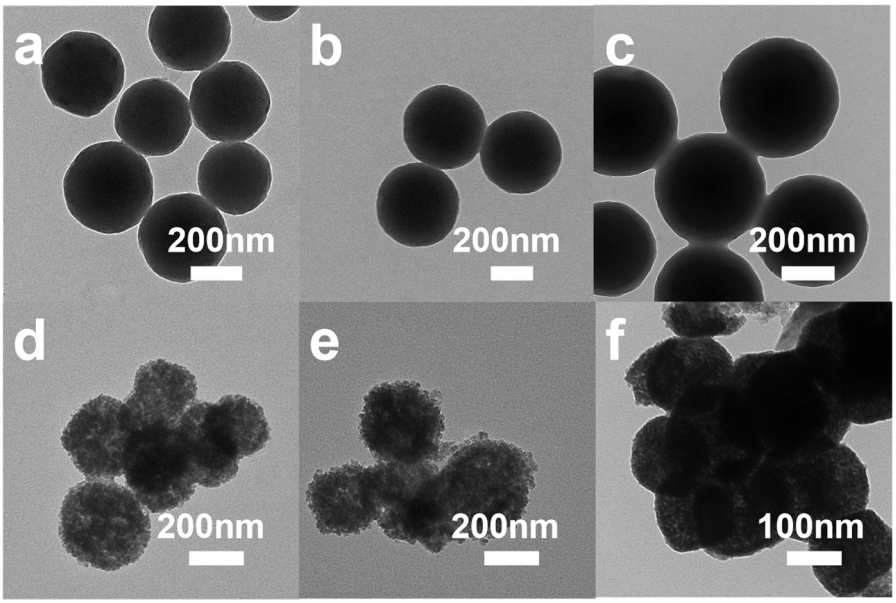

Figure S32 TEM images of (a) CoCeNi-CDSAAs-1, (b) CoCeNi-CDSAAs-2, (c) CoCeNi-CDSAAs-4, (d) $CoCeNiO_x$-1, (e) $CoCeNiO_x$-2 and (f) $CoCeNiO_x$-4.

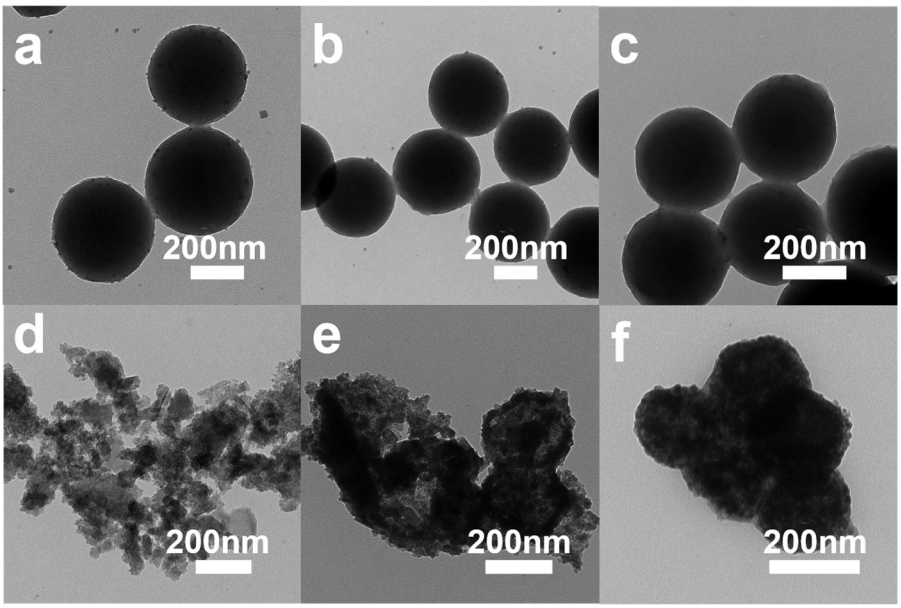

Figure S33 TEM images of (a) CoCeEr-CDSAAs-1, (b) CoCeEr-CDSAAs-2, (c) CoCeEr-CDSAAs-4, (d) $CoCeErO_x$-1, (e) $CoCeErO_x$-2 and (f) $CoCeErO_x$-4.

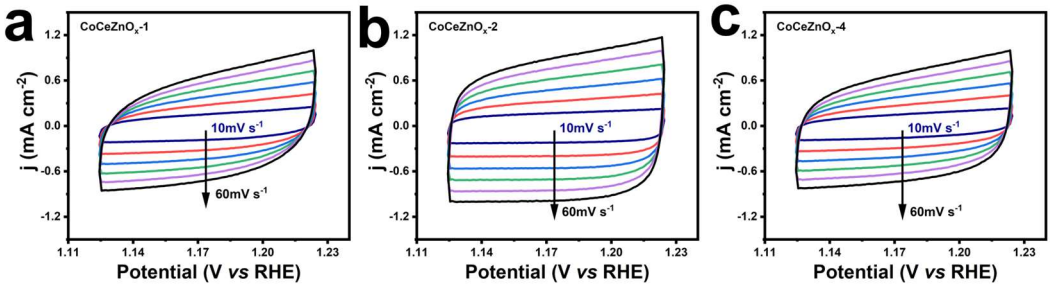

Figure S34 CV curves of (a) $CoCeZnO_x$-1, (b) $CoCeZnO_x$-2 and (c) $CoCeZnO_x$-4 with different scan rates from 10 to 60 mV s^{-1}.

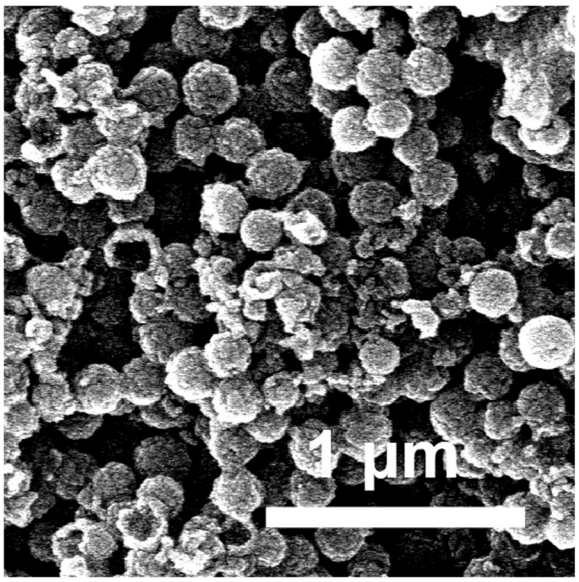

Figure S35 SEM image of $CoCeZnO_x$ after CP test corresponding to the EDX selection area.

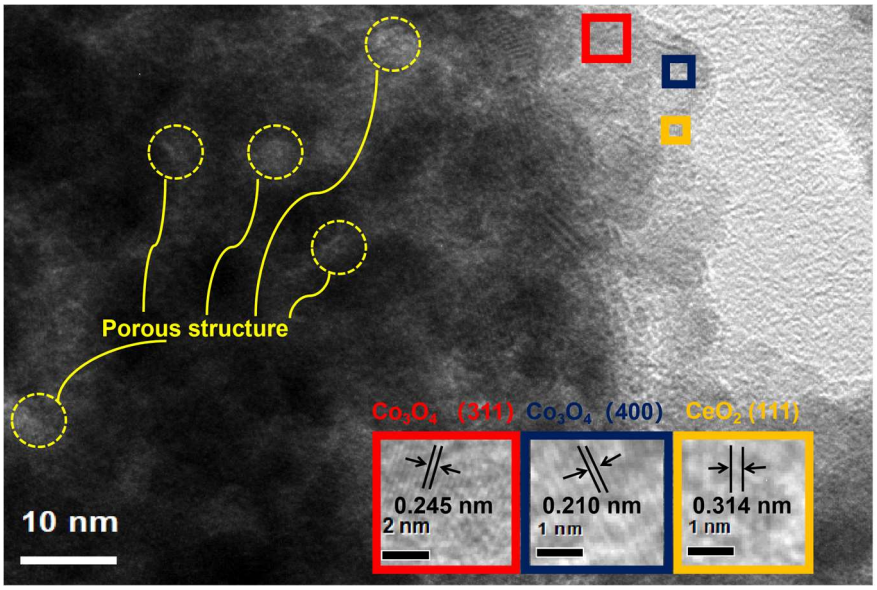

Figure S36 HRTEM image of $CoCeZnO_x$ after CP test.

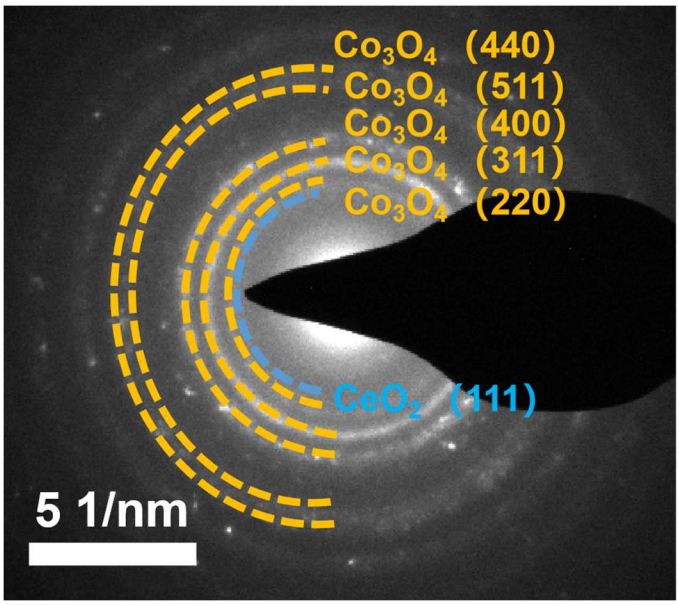

Figure S37 SAED image of $CoCeZnO_x$ after CP test.

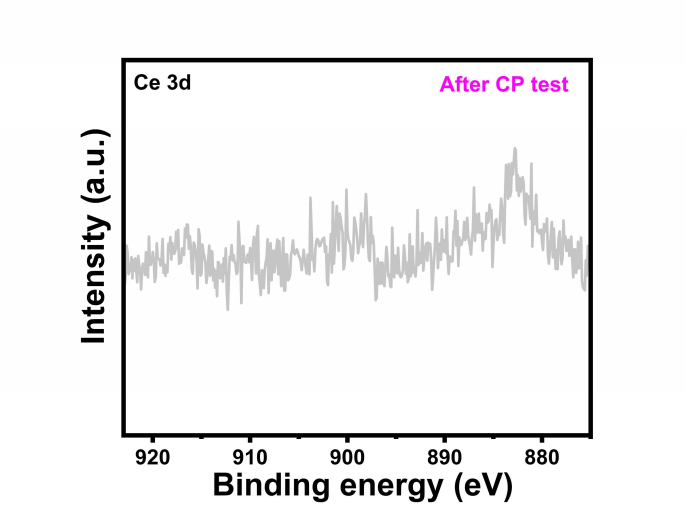

Figure S38 Ce 3d high-resolution XPS spectra in $CoCeZnO_x$ PNs after CP test.

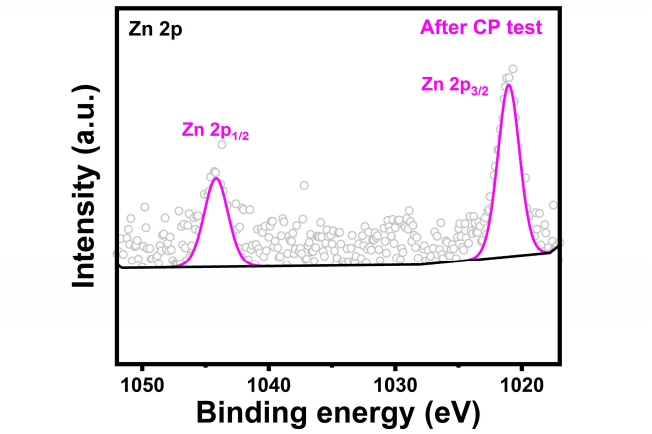

Figure S39 Zn 2p high-resolution XPS spectra in $CoCeZnO_x$ PNs after CP test.

Table S1 Comparison of the OER performance of $CoCeZnO_x$ PNs with previously reported Co-based OER electrocatalysts in 1M KOH solution.

Catalysts	η (10mA cm^{-2}) (mV)	Reference
$CoCeZnO_x$ PNs	333	This Work
Ni/Co_3O_4@NC	350	1
C-Co/Co_3O_4 hollow sphere	352	2
Ce-Co_3O_4	369	3
Co-MOF-CSMSs	350	4
In-Co_3O_4	340	5
LDH-R@Co(v-Zn)-NCNTs	344	6

Reference

1 B. Dong, J. Xie, Z. Tong, J. Chi, Y. Zhou, X. Ma, Z. Lin, L. Wang and Y. Chai, *Chinese J. Catal*., 2020, **41**, 1782–1789.

2 L. Hang, Y. Sun, D. Men, S. Liu, Q. Zhao, W. Cai and Y. Li, *J. Mater. Chem. A*, 2017, **5**, 11163–11170.

3 X. Huang, H. Zheng, G. Lu, P. Wang, L. Xing, J. Wang and G. Wang, *ACS Sustainable Chem. Eng*., 2018, **7**, 1169-1177.

4 P. Liu, H. Han, Q. Xia, N. Ma, S. Lu, X. Shang, G. Wang and S. Chao, *Dalton Trans*., 2021, **50**, 11440–11445.

5 Z. Shao, X. Gao, Q. Zhu, W. Zhao, X. Wu, K. Huang and S. Feng, *Chem. Commun*., 2022, **58**, 10408–10411

6 W. Yang, Y. Bai, J. Ma, Z. Wang, W. Sun, J. Qiao, H. Cai and K. Sun, *J. Mater. Chem. A*, 2020, **8**, 25268–25274.